Study of the Micellization Behavior of Different Order Amino Block Copolymers with Heparin

Marie-Hélène Dufresne[1] and Jean-Christophe Leroux[1,2]

Received September 2, 2003; accepted September 30, 2003

Purpose. The purpose of this study was to prepare and characterize copolymers presenting different pendant amino groups and to study their ability to form polyelectrolyte complexes with heparin. The responsiveness of the complexes to variations in pH and ionic strength was correlated to the nature of the copolymers.

Methods. Copolymers composed of different aminoethyl methacrylate monomers were synthesized by atom transfer radical polymerization (ATRP) from a poly(ethylene glycol) macroinitiator. Copolymers were characterized by gel permeation chromatography and nuclear magnetic resonance spectroscopy. Micellization properties were assessed by atomic force microscopy, multiangle static light scattering, and dynamic light scattering on complexes formed from the addition of heparin to a solution of polymer.

Results. Primary, tertiary, and quaternary amine-based diblock copolymers with molecular weights ranging from 4900 to 7400 and low polydispersity indexes were prepared. The synthesis of a copolymer bearing primary amines was achieved for the first time by ATRP. Micellization was found to be pH- and polymer-dependent. All polymers interacted with heparin at acidic pH to yield monodisperse assemblies of less than 30 nm. Complexes dissociated in response to increases in ionic strength.

Conclusions. Electrostatic interactions between the amino copolymers and heparin triggered the formation of small, monodisperse, and stable complexes that present great potential as oral drug delivery systems.

KEY WORDS: atom transfer radical polymerization; cationic copolymers; heparin; polyion complex micelles.

INTRODUCTION

Heparin is a macromolecular glycosaminoglycan with anticoagulant properties. It is one of the drugs most widely used in North America for preventing and treating deep vein thrombosis and pulmonary embolisms. Unfortunately, its administration is restricted to the parenteral route as its oral bioavailability is impaired by a short half-life, large molecular size, and overall negative charge. Current treatments require careful patient monitoring and therefore point to the development of new lower-cost and patient-friendly formulations. Several strategies have been explored to increase the oral bioavailability of heparin. These are generally aimed either at the neutralization of its negative charges (to prevent electrostatic repulsions between the drug and gastrointestinal mucosa) or the protection of the drug from pH and enzymatic degradation. Examples include the use of absorption enhancers [such as ethylenediaminetetraacetic acid (1) or sulfonated surfactants (2)], chemical modifications [deoxycholic acid–heparin conjugates (3)], and particulate carrier systems (4). However, these approaches have only had limited success. Currently, the most effective formulation is the coadministration of heparin with *N*-[8-(2-hydroxybenzoyl)amino]caprylate (5), an absorption enhancer that improves the oral absorption of heparin in humans. Though promising, this formulation is not yet optimal in that the anticoagulant activity only lasts 4 h at doses higher than those usually recommended for humans. Recently, the use of polymeric carriers has attracted considerable attention as the technology can simultaneously protect a drug from the surroundings, provide a controlled and sustained release, and potentially account for increased absorption. In this light, heparin-loaded micro- and nanoparticles composed of blends of two biodegradable polymers [namely poly(∈-caprolactone) and poly(D,L-lactic-*co*-glycolic acid)] and two nonbiodegradable cationic polymethacrylates (Eudragit RS and RL) were proposed by Maincent and co-workers (6,7). These systems presented anticoagulant activity in a rabbit model for up to 7 h at doses close to those commonly administered by the intravenous route. We now intend to exploit the properties of polymeric carrier systems by introducing a new formulation of heparin as polyion complex micelles (PICM).

PICM generally result from favorable interactions between a charged diblock copolymer and an oppositely charged polyion (8). The formation of PICM is best described as the sequential complexation of the polyions through electrostatic interactions followed by the self-association of the condensates into micelles. Neutralization of the charged segments indeed yields water-insoluble moieties that contribute to a decrease in the entropy of the system. To offset this entropy loss, the neutralized segments withdraw from the aqueous phase and self-assemble into micelles presenting a core/shell architecture. The formation of PICM was shown to be concentration-dependent, and the critical association concentration of such systems has been evaluated by either monitoring changes in the intensity of pyrene fluorescence emission (9) or in the apparent molecular weight (10) with concentration. PICM have been designed for the delivery of charged drugs such as oligonucleotides (11), DNA (12), and enzymes (13). They present numerous advantages including their straightforward synthesis, self-assembly in aqueous medium, and narrow size distribution. Furthermore, entrapment of the drug in the core was shown to protect it from *in vivo* metabolism or enzymatic degradation (10). Polymers commonly used for the delivery of polyanionic drugs include poly-

[1] Canada Research Chair in Drug Delivery, Faculty of Pharmacy, University of Montreal, P.O. Box 6128, Succ. Centre-Ville, Montreal, Quebec, Canada, H3C 3J7.

[2] To whom correspondence should be addressed. (e-mail: jean-christophe.leroux@umontreal.ca)

ABBREVIATIONS: α, ionization degree; AEMA, 2-(*N*-amino)ethyl methacrylate hydrochloride; AEMABoc, 2-[*N*-(*tert*-butoxycarbonyl) amino]ethyl methacrylate; AFM, atomic force microscopy; ATRP, atom transfer radical polymerization, $CDCl_3$, deuterated chloroform; CD_3OD, deuterated methanol; D_2O, deuterated water; DCM, dichloromethane; DEAEMA, 2-(*N*,*N*-diethylamino)ethyl methacrylate; DEMAEMA, 2-(*N*,*N*,*N*-diethylmethylamino)ethyl methacrylate; DLS, dynamic light scattering; DMAEMA, 2-(*N*,*N*-dimethylamino) ethyl methacrylate; GPC, gel permeation chromatography; ^{1}H NMR, proton nuclear magnetic resonance; MASLS, multiangle static light scattering; M_n, number-average molecular weight; M_w, weight-average molecular weight; MW, molecular weight; PAMAM, polyamidoamide; PEG, poly(ethylene glycol); PEI, polyethyleneimine; PI, polydispersity index; PICM, polyion complex micelles; PMDETA, *N*,*N*,*N'*,*N'*,*N''*-pentamethyldiethylenetriamine; THF, tetrahydrofuran; TMAEMA, 2-(*N*,*N*,*N*-trimethylamino)ethyl methacrylate.

0724-8741/04/0100-0160/0 © 2004 Plenum Publishing Corporation

ethylenimine (PEI) (14), poly(L-lysine) (11), polyamidoamide (PAMAM) (15), and poly[2-(*N*,*N*-dimethylamino) ethyl methacrylate] (PDMAEMA) (16). All polymers, except for PDMAEMA, present primary amines that are mostly protonated at physiological pH. Furthermore, PEI and PAMAM possess higher order amines that are responsible for their increased buffering capacity. Clearly, the order (i.e., degree of substitution) of the amines confers certain characteristic properties to the drug–polymer complexes. In this study, block copolymers of poly(ethylene glycol) (PEG) and moieties bearing different amino groups (Fig. 1) were synthesized in order to evaluate the relationship between the different order amines and their complexation behavior with heparin. The polymerization of different alkylated derivatives of 2-(*N*-amino)ethyl methacrylate provided a range of primary, tertiary, and quaternary amine-based complexes.

All copolymers were synthesized by a robust and versatile controlled polymerization method known as atom transfer radical polymerization (ATRP). ATRP allows for the control of molecular weight and polydispersity of polymer chains as well as their composition (17), architecture (18), and end-group functionality (19). The success of ATRP lies in the establishment of a dynamic equilibrium between propagating radicals and dormant polymer chains so as to keep the actual concentration of active species much lower than the total concentration of chains, thus reducing radical–radical termination and enhancing control over the polymerization reaction (20). Despite its capability of polymerizing a wide range of monomers, the polymerization of methacrylates presenting pendant amino groups remains difficult. This is because amines can provoke the displacement of the ligand from the metal complex (21) and, in the case of primary amines, react with the halogen end group of the initiator or of the growing polymer chain (19). Under appropriate reaction conditions, we were able to exploit ATRP for the synthesis of copolymers presenting different amino groups. To the best of our knowledge, this is the first report in which ATRP was successfully used to produce polymers bearing pendant primary amino groups.

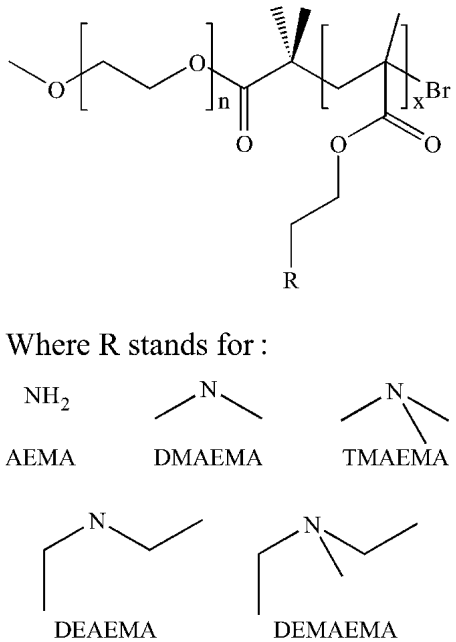

Fig. 1. Structure of the amino diblock copolymers studied.

MATERIALS AND METHODS

Materials

Heparin sodium salt from porcine intestinal mucosa [molecular weight (MW) of ~6000] was purchased from Sigma (St. Louis, MO, USA). 2-(*N*-amino)ethyl methacrylate hydrochloride (AEMA) was obtained from Polysciences Inc. (Warrington, PA, USA) and used as received. All other chemicals were purchased from Aldrich Chemical Co. (Milwaukee, WI, USA) and used as received, except for 2-(*N*,*N*-dimethylamino)ethyl methacrylate (DMAEMA) and 2-(*N*,*N*-diethylamino)ethyl methacrylate (DEAEMA), which were vacuum-distilled prior to polymerization. Tetrahydrofuran (THF) was dried over sodium with benzophenone as indicator, and dichloromethane (DCM) was dried over calcium chloride.

Instrumentation

Nuclear Magnetic Resonance Analyses

All ^{1}H NMR spectra were recorded on a Bruker NMR spectrometer operating at 300 MHz (Bruker, Milton, Ontario, Canada). Solutions were prepared in deuterated chloroform ($CDCl_3$), methanol (CD_3OD), or water (D_2O).

Molecular Weight Determination

Number- (M_n) and weight-average (M_w) MWs were determined by gel permeation chromatography (GPC) using an Alliance GPCV 2000 system (Waters, Milford, MA, USA) equipped with a differential refractive index detector. GPC analyses were performed in THF (HPLC grade) using three Waters Styragel columns (HR1, HR3, and HR4) in series at a flow rate of 1.0 ml/min and a temperature of 40°C. A calibration curve was obtained with near-monodisperse PEG standards.

Dynamic Light Scattering and Multiangle Static Light Scattering Measurements

The mean hydrodynamic diameter, size distribution, and scattering intensity of PICM were determined using a Malvern Autosizer 4800 equipped with a 488-nm uniphase argon–ion laser (Malvern Instruments, Worcestershire, UK). Measurements were performed in triplicate at a scattering angle of 90° and a temperature of 25°C. The CONTIN program was used to extract size distributions from the autocorrelation functions. Alternatively, MASLS measurements were conducted at 25°C at eight angles ranging from 50° to 120° for a minimum of three concentrations. All samples were passed through 0.45- and 0.22-μm nylon filters prior to analysis. The M_ws of the complexes were extracted from Eq. (1), which describes the intensity of light scattered from a dilute solution of macromolecules:

$$\frac{Kc}{R_0} = \frac{1}{M_w P(\theta)} + 2A_2c + 3A_3c^2 \quad (1)$$

In this equation, c stands for the solution concentration in both polymer and heparin, R_0 is the Rayleigh ratio of the

solution, and A_2 and A_3 are the second and third virial coefficients. K is in turn defined by:

$$K = \frac{4\pi^2 n_0^2 \left(\frac{dn}{dc}\right)^2}{\lambda^4 N} \quad (2)$$

where n_0 is the refractive index of the solvent, λ the laser wavelength *in vacuo*, and N Avogadro's number. The specific refractive index increments (dn/dc) were determined using a differential Rudolph J157 automatic refractometer (Rudolph Research Analytical, Flanders, NJ, USA), at a wavelength of 589.3 nm.

Atomic Force Microscopy Imaging

The topographic data of the complexes was collected using a Nanoscope III Dimension 3100 atomic force microscope (Digital Instruments, Santa Barbara, CA, USA). Imaging was performed in tapping mode with a silicon tip (tapping mode etched Si probes – RTESP7) operating at a 300-kHz resonant frequency and a 42 N/m constant force. Samples were prepared by letting a drop of an acidic aqueous solution of PICM (polymer concentration of 0.2 mg/ml, pH 5) dry on a freshly cleaved mica surface at room temperature. PICM were formed at a –/+ molar charge ratio of 1.5.

Synthesis of Poly(Ethylene Glycol) ATRP Macroinitiator [α-(2-Bromoisobutyrylate)-ω-MethylPEG]

Fifteen grams of MeO–PEG–OH (M_n = 2000, 7.5 mmol) was dried with toluene by azeotropic distillation, dissolved in 70 ml anhydrous THF, and chilled for 20 min in an ice-water bath in presence of triethylamine (2.4 ml, 17.2 mmol). 2-Bromoisobutyryl bromide (6.5 ml, 33.5 mmol) was added dropwise; the reaction mixture was warmed to room temperature and allowed to react for 48 h (22). The reaction was stopped by adding DCM and washing with 10% aqueous HCl. The organic phase was then extracted with 1 M NaOH, brine, and dried over magnesium sulfate. Solvents were evaporated under reduced pressure. The crude extract was dissolved in a minimum of DCM and precipitated in diethyl ether. The product was recovered by simple filtration.

^{1}H NMR (δ, ppm, $CDCl_3$): 4.33 (2H, t), 3.65 (180H, m), 3.38 (3H, s), 1.94 (6H, s). Yield: 70%, after precipitation.

Synthesis of 2-[*N*-(*tert*-Butoxycarbonyl)Amino]Ethyl Methacrylate (AEMABoc)

A suspension of AEMA in anhydrous DCM (0.30 M) was stirred for 10 min in an ice-water bath. Freshly distilled triethylamine was then added (1.1 Eq) and the reaction mixture stirred for 20 min. A solution of bis(*tert*-butyl)dicarbonate in DCM (1.1 Eq in sufficient DCM to bring AEMA to a final concentration of 0.27 M) was added; the reaction mixture was warmed to room temperature and allowed to react for 24 h. The reaction was stopped by extracting the organic phase with water, 1 M HCl, saturated aqueous sodium bicarbonate, and brine. The organic extract was dried over sodium sulfate, and the solvent was removed *in vacuo* to give a crude crystalline product that was used without further purification.

^{1}H NMR (δ, ppm, $CDCl_3$): 6.13 (1H, d), 5.60 (1H, t), 4.78 (1H, broad s), 4.21 (2H, t), 3.45 (2H, q), 1.95 (3H, s), 1.45 (9H, s). Yield: 93%.

ATRP Polymerization

Polymerization of monomers was performed in solution using α-(2-bromoisobutyrylate)-ω-methylPEG as the ATRP macroinitiator. The PEG ATRP macroinitiator (1 Eq) was dissolved in distilled THF along with 16–25 Eq of the monomer to a final monomer concentration of 0.5 or 0.8 M. Concurrently, Cu(I)Br (1.1 Eq) and *N*,*N*,*N'*,*N'*,*N''*-pentamethyldiethylenetriamine (PMDETA, 1.1 Eq) were mixed in a second round-bottom flask. The contents of both reaction vessels were purged with argon for 15–20 min, after which the PEG–monomer solution was transferred to the metal complex activator using a two-head syringe. Polymerization was typically carried out at 65°C for 16 h. The polymerization reaction was stopped by dilution with an ethanol–THF solution (final ethanol concentration of 10%) and removal of the copper complex by filtration on a silica gel column using THF as eluent. Evaporation of the solvents under reduced pressure provided crude polymers that were purified by dialysis against water (Spectra/Por no.1, MW cut-off 6000–8000) for at least 48 h and recovered by freeze-drying (using a FreeZone 6 system, Labconco, Kansas City, MO, USA).

PEG-b-P(AEMABoc)

^{1}H NMR (δ, ppm, $CDCl_3$): 5.54 (16H, broad s), 4.01 (32H, broad s), 3.65 (185H, m), 3.39 (3H, s + 32H, broad s), 1.84 (36H, m), 1.45 (160H, s), 1.26–0.89 (6H, s + 46H, m).

PEG-b-P(DMAEMA)

^{1}H NMR (δ, ppm, $CDCl_3$): 4.08 (33H, broad s), 3.65 (176H, m), 3.38 (3H, s), 2.59 (33H, broad s), 2.30 (96H, s), 1.98–1.83 (31H, m), 1.14–0.90 (6H, s + 46H, m). Yield: 25%, after purification.

PEG-b-P(DEAEMA)

^{1}H NMR (δ, ppm, $CDCl_3$): 3.99 (25H, broad s), 3.65 (175H, m), 3.39 (3H, s), 2.70 (25H, broad s), 2.58 (50H, m), 1.98–1.81 (24H, m), 1.26–0.90 (6H, s + 77H, t + 39H, m). Yield: 31%, after purification.

Deprotection of PEG-*b*-P(AEMABoc) to Its Hydrochloride Salt Derivative PEG-*b*-P(AEMA)

Crude polymer extracts were dissolved in 3 M HCl/EtOAc to a final amine concentration of 0.15 N. The reaction was carried out for 2½ h after which solvents were removed under reduced pressure. The polymer was dissolved in ethanol, dialyzed against water, and recovered by freeze-drying.

^{1}H NMR (δ, ppm, D_2O): 4.21 (34H, broad s), 3.66 (165H, m), 3.34 (3H, s), 3.25 (34H, broad s), 1.99 (31H, m), 1.16–0.90 (6H, s + 50H, m). Yield: 28%, after purification.

Transformation of PEG-*b*-P(DMAEMA) and PEG-*b*-P(DEAEMA) into PEG-*b*-Poly[2-(*N*,*N*,*N*-Trimethylamino)Ethyl Methacrylate] [PEG-*b*-P(TMAEMA)] and PEG-*b*-Poly[2-(*N*,*N*,*N*-Diethylmethylamino)Ethyl Methacrylate] [PEG-*b*-P(DEMAEMA)], Respectively

Alkylation of the tertiary amine groups of the methacrylate residues was done in order to introduce permanent positive charges on the nitrogen atoms. An excess of methyliodide (2 Eq with respect to amino groups) was added to a solution of polymer in water (30 mg/ml). Methylation was carried for 3 and 4 h for PEG-*b*-P(DMAEMA) and PEG-*b*-P(DEAEMA), respectively. The quaternized polymers were purified by dialysis against water and recovered by freeze-drying.

PEG-b-P(TMAEMA)

^{1}H NMR (δ, ppm, CD_3OD): 4.56 (33H, broad s), 4.09 (32H, broad s), 3.64–3.36 (181 H, m + 150 H, broad s + 3H, s), 2.07 (32H, broad s), 1.31–1.06 (6H, s + 51H, m). Yield: 76%, after purification.

PEG-b-P(DEMAEMA)

^{1}H NMR (δ, ppm, CD_3OD): 4.54 (24H, broad s), 3.96 (24H, broad s), 3.64 (47H, broad s + 170H, m), 3.36 (3H, s), 3.31 (CD_3OD + broad s), 2.06 (24H, broad s), 1.47 (72H, broad s), 1.23–1.09 (6H, s + 37H, m). Yield: 59%, after purification.

Potentiometric Titrations

Titration curves were generated by first titrating the polymer solutions (1 mg/ml) to low pH using 0.01 N HCl to ensure complete dissolution of the polymers. Changes in pH values were then monitored with a portable Accumet AP61 pH-meter (Fisher Scientific, Montreal, Qc, Canada) following incremental additions of a standardized 0.01 N NaOH solution. The apparent pK_a values were calculated from Eq. (3):

$$pK_a = pH - \log\left(\frac{1-\alpha}{\alpha}\right) \quad (3)$$

α is defined as the ratio C_{N+}/C_m, where C_{N+} stands for the effective concentration of protonated amino groups and C_m is the monomeric concentration in methacrylates. Assuming that all added hydroxide ions are able to deprotonate the amine groups, a fair approximation of C_{N+} is calculated using the effective concentration of NaOH added (23).

Effect of Heparin/Polymer Molar Charge Ratio on Micelle Formation

Specific amounts of a concentrated heparin solution (60 mg/ml) were added to a solution of polymer (5 mg/ml) in an acetate buffer (16.6 mM sodium acetate, 83.4 mM acetic acid, pH 4) to yield complexes with –/+ molar charge ratios varying from 0 to 2.95. The density of charges on heparin was assumed to be of 5 mEq/g. DLS analyses were performed after each incremental addition of heparin. Both the stock heparin and polymer solutions were passed through 0.22-μm nylon filters prior to experimentation.

Effect of pH on Micelle Formation

PICM of heparin (–/+ molar charge ratio of 1.5) were prepared to final polymer concentrations of 1 mg/ml. The pH of the preparations was acidified with 1 N HCl to ~4 and sequentially increased to ~11 using 1 N NaOH. Aliquots were sampled after each incremental addition of NaOH, passed through 0.45-μm filters, and analyzed by DLS. Size data was only recorded for samples with high enough scatter counts (above the detection limit).

Effect of Salt Concentration on Micelle Stability

Stoichiometric PICM of heparin were prepared as acidified aqueous solutions (pH ~4) with final polymer concentrations of 5–7.5 mg/ml. Specific volumes of a 5 M NaCl solution were added to yield solutions with salt concentrations ranging from 0 to 1.2 M. Both the PICM and stock salt solutions were passed through 0.45-μm nylon filters. DLS analyses were performed after each incremental addition of salt. Size data was only recorded for samples with high enough scatter counts (above the detection limit).

Effect of Freeze-Drying on PICM Integrity

Stoichiometric PICM of heparin were prepared in an acetate buffer (67.8 mM sodium acetate, 32.2 mM acetic acid, pH 5) to final polymer concentrations of 2.5 mg/ml. Comparatively, stoichiometric PICM of heparin were prepared as acidified aqueous solutions (pH ~5) with final polymer concentrations of 2.5 mg/ml. Solutions were passed through 0.45-μm nylon filters prior to initial DLS analysis. The samples were then frozen overnight at –80°C and freeze-dried for 48 h. Changes in micelle size were evaluated by DLS after resuspension of the dried cakes in deionized water.

RESULTS AND DISCUSSION

Polymer Synthesis

ATRP is a radical polymerization method that allows the preparation of polymers with controlled and diverse compositions. Its success lies in its ability to combine fast initiation rates with low concentrations of propagating radicals. This critical equilibrium between growing radicals and dormant species is a function of the nature of the transition metal–ligand catalyst complex used. It then becomes of crucial importance that the species to be reacted do not interfere with the ATRP equilibrium. Accordingly, the polymerization of methacrylates presenting pendant amino groups becomes challenging for two reasons. First, displacement of the ligand on the metal complex by the growing polymer chain could occur. ATRP ligands often present amino groups used for coordination to the metal catalyst; monomers bearing amines are direct competitors to the ligand and can disturb the sensitive metal–ligand equilibrium. This problem can be overcome by using polydentate ligands (21), given that their chelating effect confers them an enhanced stability. PMDETA is one such polydentate ligand and was selected as it presents both fast rates of activation and deactivation, thus rendering its metal complexes very active catalysts (24). Second, side reactions between the free amines and the halogen end group of the macroinitiator and/or growing polymer chain are to be

anticipated. Coessens *et al.* (19) have shown that bromide end groups are available for nucleophilic substitution reactions to yield polymers with amino end groups. These authors additionally revealed that under the experimental conditions used during typical ATRP processes, interactions of the end bromine group with tertiary amines were negligible whereas they could take place with primary amines. The combination of these adverse interactions advocates that great care must be taken during the ATRP of amine-bearing monomers and calls for the protection of the primary amine groups. In this light, the *tert*-butoxycarbonyl (Boc) protective group was introduced on AEMA prior to its polymerization. Boc was selected as it reduces the accessibility of the lone amine electron pair through both steric hindrance and its electron-withdrawing activity. Furthermore, Boc can easily be cleaved under mild acidic condition (3 M HCl/EtOAc), leaving the ester bonds of the polymer intact. Under proper reaction conditions, ATRP allowed for the preparation of well-defined cationic copolymers originating from a PEG-based unit.

Characterization of Diblock Copolymers

The MW characteristics and polydispersity indexes (PIs) of the polymers are reported in Table I. M_ns were evaluated by ^{1}H NMR from the integration of the two methylene groups of the pendant aminoethyl segments with respect to that of the methoxy group of the PEG macroinitiator. The ^{1}H NMR spectra of PEG-*b*-P(AEMABoc) and its derivative PEG-*b*-P(AEMA) are shown as examples in Fig. 2. Figure 2B confirms the complete deprotection of the primary amine through the disappearance of the peak at 1.45 ppm (assigned to the Boc *tert*-butyl group). Note that the –$N\underline{H}_2$ signal is lost given that these protons are easily exchanged with the surrounding deuterated solvent (D_2O). M_ns were also determined by GPC relative to PEG standards. MWs calculated from both techniques reasonably correlated, with the GPC results being invariably underestimated. GPC analyses further allowed for the evaluation of PIs. PIs were relatively low ($\leq$1.23), as expected for controlled polymerization processes. Table I additionally reveals that the reaction conditions [i.e., in presence of the Cu(I)Br/PMDETA complex at 65°C in THF] are suitable for the polymerization of both the AEMABoc and DMAEMA derivatives but are inadequate for DEAEMA; degrees of conversion of PEG-*b*-P(DEAEMA) are maximized at ~80–88% of the feed.

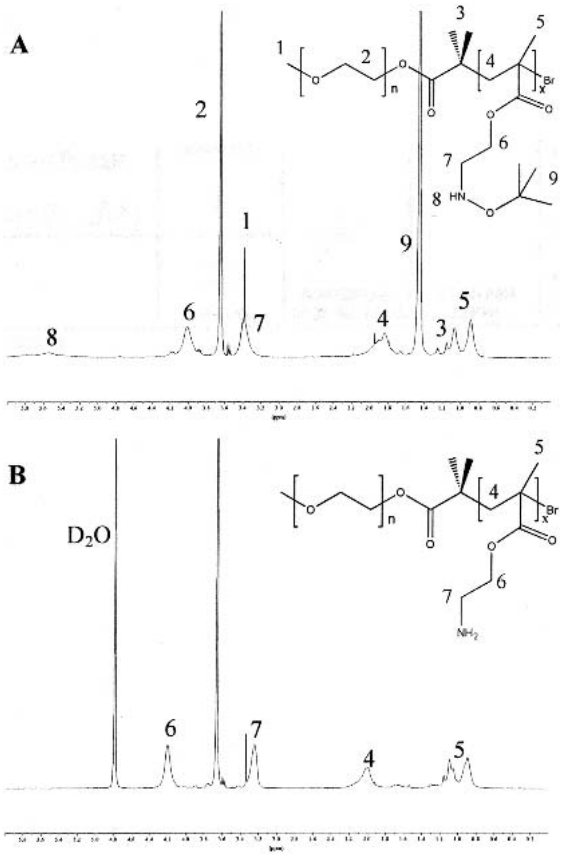

Fig. 2. ^{1}H NMR spectra of (A) diblock copolymer PEG-*b*-P(AEMABoc) in $CDCl_3$ and (B) of its deprotected equivalent PEG-*b*-P(AEMA) in D_2O.

Potentiometric Titrations

PEG-*b*-P(TMAEMA) and PEG-*b*-P(DEMAEMA) copolymers were not titrated as their amino groups are quater-

Table I. Characteristics of the Diblock Copolymers and Their Heparin-Based PICM

Description	M_n[a] (theo)	M_n[b] (NMR)	M_n[c] (GPC)	PI[d]	Conversion degree ($M_{n,NMR}$/$M_{n,theo}$)	PICM diameter (nm)[e] [PI]	PICM MW[e]	Aggregation number[f]	Rehydrated PICM diameter (nm)[e] [PI]
PEG-*b*-P(AEMA)[g]	5800	5800	3800	1.17	1.00	24.7 [0.159]	340,000	41	24.2 [0.160]
PEG-*b*-P(DMAEMA)	4700	4900	3900	1.23	1.04	30.8 [0.110]	446,000	53	44.3 (19.9%) 189.6 (83.1%)[h]
PEG-*b*-P(TMAEMA)	6900	7400	—	—	1.07	30.6 [0.080]	496,000	45	35.4 [0.193]
PEG-*b*-P(DEAEMA)	5100	4500	4700	1.16	0.88	32.4 [0.147]	692,000	80	342.1 [1.000]
PEG-*b*-P(DEMAEMA)	7400	5900	—	—	0.80	31.6 [0.086]	380,000	40	40.2 [0.301]

PICM, polyion complex micelles; M_n, number-average molecular weight; PI, polydispersity index; MW, molecular weight; theo, theoretical.
[a] Calculated from feed composition.
[b] Evaluated by ^{1}H NMR.
[c] Evaluated by GPC relative to PEG standards.
[d] Polydispersity index derived using MWs obtained by relative analysis.
[e] Stoichiometric PICM were prepared in an acetate solution (pH 5.0).
[f] The aggregation number refers to the number of polymer chains per micelle and was calculated by dividing the PICM MW by the average MW of a single stoichiometric polymer–heparin condensate.
[g] MW data is that of PEG-*b*-P(AEMABoc) whereas the PICM were synthesized using PEG-*b*-P(AEMA).
[h] Numbers in parentheses represent the population distribution. PIs were not available.

nized. Figure 3A illustrates the variations in pH expressed against α for the PEG-*b*-P(AEMA), PEG-*b*-P(DMAEMA), and PEG-*b*-P(DEAEMA) copolymers. The copolymers all behave as weak bases and present buffering capacities, as evidenced by the presence of plateaus. pK_a values were directly extracted from the titration curves and correspond to the pH value at $\alpha = 0.5$. pK_as of 7.13 ± 0.01, 6.58 ± 0.07, and 6.75 ± 0.02 were obtained for the conjugate acids of PEG-*b*-P(AEMA), PEG-*b*-P(DMAEMA), and PEG-*b*-P(DEAEMA), respectively. pK_a values measured for PEG-*b*-P(DMAEMA) and PEG-*b*-P(DEAEMA) are in agreement with those found in the literature (23,25). These results indicate that PEG-*b*-P(AEMA) should form polyelectrolyte complexes over a broader pH range as it is the most basic of all three copolymers.

In a past study, Přádný and Ševčík (25) monitored the potentiometric behavior of PDMAEMA in water–ethanol solutions and observed a dependence between the apparent pK_a and α that was attributed to conformational transitions. The authors explained that as α varies from 0 to 1, the conformation of the polymeric chains changes from statistical coils to extended chains due to electrostatic repulsions between the amino groups. Figure 3B plots the apparent pK_a values of PEG-*b*-P(AEMA), PEG-*b*-P(DMAEMA), and PEG-*b*-P(DEAEMA) and illustrates their dependence on α. Both PEG-*b*-P(AEMA) and PEG-*b*-P(DMAEMA) exhibit similar curves with drops of their apparent pK_a by unity as α varies from 0 to 1. Such profiles correlate well to the classical coiled/extended transition brought about by the ionization of the amino groups. However, divergences were observed for the PEG-*b*-P(DEAEMA) copolymer. The apparent pK_a vs. α curve presented a plateau in the region of neutrality (i.e., up to 18% ionization) indicating that no conformational changes took place. This can be rationalized by the fact that the DEAEMA segments are sufficiently hydrophobic to trigger the self-association of the block copolymer chains into micelles (see section entitled "Effect of pH on Micelle Formation," below, for further details). Electrostatic repulsions ensuing from ionization of the amines eventually led to dissociation of the micelles and extension of the polymeric chains.

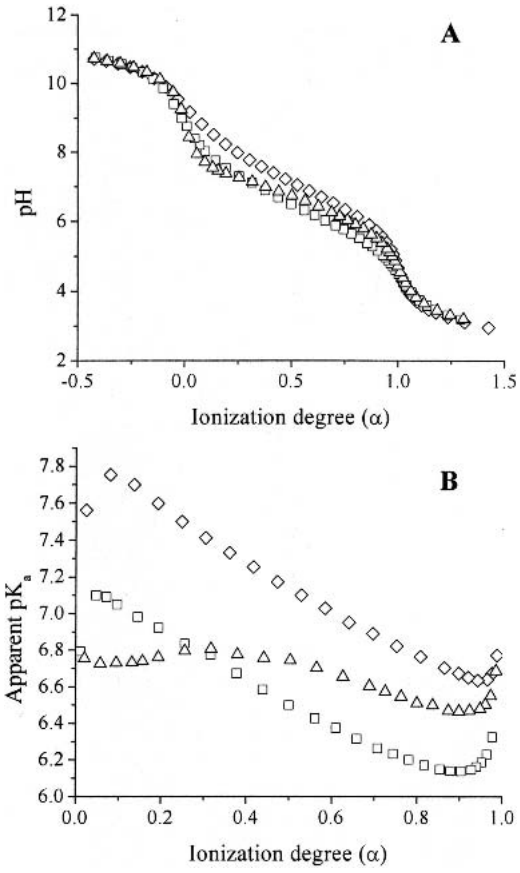

Fig. 3. (A) pH and (B) apparent pK_a of (◇) PEG-*b*-P(AEMA), (□) PEG-*b*-P(DMAEMA), and (△) PEG-*b*-P(DEAEMA) copolymers as a function of α. Polymer solutions (1 mg/ml) were first acidified with HCl and titrated with 0.01 N NaOH. Complete ionization occurs at $\alpha = 1$.

Characterization of PICM

Effect of Heparin/Polymer Molar Charge Ratio on Micelle Formation

Variations in micelle size, distribution, and scattering intensity of heparin-based PICM were monitored by DLS as a function of the heparin/polymer molar charge ratio. Complexes were prepared in acidic buffered solutions (pH 4) to ensure that every amino group of the polymers was protonated. Heparin remains ionized in these conditions given that its least acidic group has a pK_a of 3.13 (26). Figure 4A specifically illustrates the dependence of PEG-*b*-P(AEMA) PICM on the heparin feed. This titration profile was roughly subdivided into three main regions, the first of which corresponds to an excess of polymer (domain I). The initial scattering intensity (drug-free polymer solution) was very low, indicating that the polymer was soluble in water and that its chains existed as unimers. Addition of heparin slowly led to increases in both particle size and scattering intensity. This behavior is supportive of a mechanism where micelle formation is driven by electrostatic interactions. Careful examination of these first assemblies most often revealed the presence of two populations and was associated to high PIs. It is as if both free polymeric chains and PICM coexisted simultaneously.

Subsequent addition of heparin eventually resulted in a domain of near stoichiometry (domain II). In this region, every ionized polymer and heparin units electrostatically interacted to yield neutral PICM with narrow size distributions. PIs lower than 0.1 were observed and confirmed that the PICM were evenly distributed and monodisperse. A typical representation of the scattering measurements is presented in Fig. 4B and illustrates the narrowness of the size distribution of the complexes. An AFM image of the PEG-*b*-P(AEMA)–heparin complexes is presented in Fig. 5. It can be seen that the complexes most often have spherical shapes (~20 nm) and that their size distribution is narrow. The MW and aggregation number of similar stoichiometric assemblies were evaluated by MASLS (Table I). It was found that PICM were composed of 40–80 polymer chains and that the aggregation number increased with increasing hydrophobicity of the monomeric core units.

The third region of the heparin titration profile (Fig. 4A) in turn corresponded to the situation where a marked excess in heparin was met (domain III). Increases in the ratio of heparin progressively induced a decrease in micelle size (data

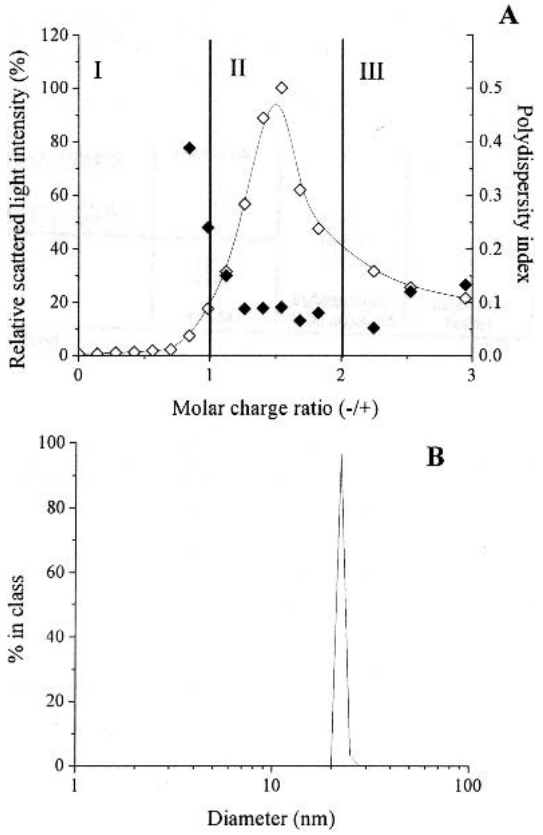

Fig. 4. (A) Effect of heparin/polymer molar charge ratio on (◇) the scattering intensity and (◆) polydispersity index of micelles prepared in an acetate buffer of pH 4. The scattering intensity is expressed relative to the maximum scattering count observed. The curve was further subdivided in three regions corresponding respectively to domains of (I) excess polymer, (II) near stoichiometry, and (III) excess heparin. (B) A typical size distribution of stoichiometric PEG-*b*-P(AEMA)–heparin PICM prepared in an acetate buffer of pH 4 is also shown.

not shown), and, concomitantly, scattering intensity. These micelles retained an extremely narrow size distribution and exhibited a single population, unlike micelles formed under an excess of polymer. Such observations suggest that micelle formation proceeded in a nonstoichiometric way in that the polymeric chains evenly distributed on the heparin molecules to yield assemblies with excess negative charges. Similar profiles were obtained for the titration of PEG-*b*-P(DMAEMA), PEG-*b*-P(TMAEMA), PEG-*b*-P(DEAEMA), and PEG-*b*-P(DEMAEMA) with heparin (data not presented).

Effect of pH on Micelle Formation

It was evidenced from the potentiometric titrations (Fig. 3) that the copolymers presented different basic properties. Their capability to form polyelectrolyte complexes at a given pH should therefore relate to their composition. The latter was investigated by determining the influence of pH (and α) on micelle formation. Figure 6A presents variations in scattering intensity following changes in pH for PEG-*b*-P(AEMA), PEG-*b*-P(DMAEMA), and PEG-*b*-P(DEAEMA) while variations in particle size are shown in Fig. 6B. The scattering counts of both PEG-*b*-P(AEMA) and PEG-*b*-P(DMAEMA) were low in basic environment, suggesting that their chains existed as unimers. In these conditions, the copolymers are completely unionized and are unable to interact electrostatically with heparin. Lowering the pH progressively protonated the amines and induced electrostatic interactions at a critical pH value. Micellization was translated as increases in both size and scattering intensity. This threshold pH value varies between polymers and closely correlates to the basicity of the amino groups (i.e., the pH at which they get ionized). It can be extrapolated from Fig. 3A that ionization of PEG-*b*-P(AEMA) and PEG-*b*-P(DMAEMA) begins at pH 9.4 and 8.9, respectively; these values intimately correspond to the pH at which their condensation to heparin was initiated (Fig. 6A, arrows 1 and 2). PICM were observable from that point on because both the copolymers and heparin existed as ionized species. Control measurements performed on solutions of PEG-*b*-P(AEMA), PEG-*b*-P(DMAEMA), or heparin demonstrated that the components individually existed as unimers throughout the whole pH range studied (data not shown).

PEG-*b*-P(DEAEMA) is peculiar in that pH has an effect on the self-assembly of the polymer itself (Fig. 6A). In the absence of heparin, the unionized DEAEMA units were sufficiently hydrophobic to trigger their segregation into the core of micelles (23) with diameters of ~20 nm. PEG-*b*-P(DEAEMA) chains retained their ability to form micelles up to 18% ionization (pH 7.4), after which they broke apart. This property of PEG-*b*-P(DEAEMA) greatly altered the pH-responsiveness profile of the PEG-*b*-P(DEAEMA)–heparin system. As opposed to the PEG-*b*-P(AEMA) and PEG-*b*-P(DMAEMA) copolymers, the PEG-*b*-P(DEAEMA) chains gathered, in basic conditions, into micelles from which the polyanionic heparin was most likely precluded. Acidifying the milieu gradually protonated the amino groups, allowing for the incorporation of heparin molecules and the formation of larger polyelectrolyte assemblies. Once again, the pH at which ionization of the polymer begins (pH 9.0, Fig. 3A) compares well to the pH at which electrostatic interactions appear (arrow 3).

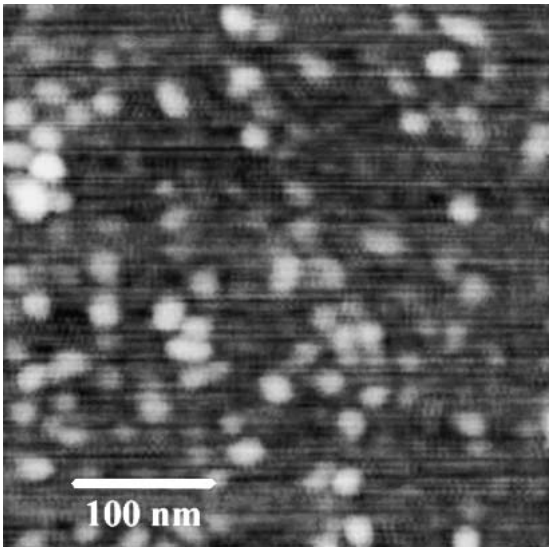

Fig. 5. AFM image of PEG-*b*-P(AEMA)–heparin PICM. Polyelectrolyte complexes were prepared as an acidified aqueous solution (pH 5) at a –/+ molar charge ratio of 1.5. Imaging was performed in tapping mode in air.

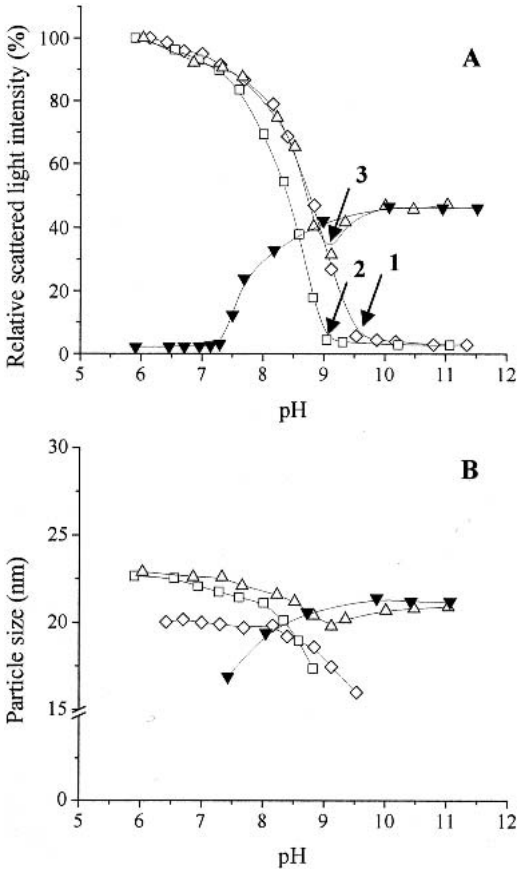

Fig. 6. Effect of pH on (A) scattering intensity and (B) particle diameter of (◇) PEG-*b*-P(AEMA), (□) PEG-*b*-P(DMAEMA), and (△) PEG-*b*-P(DEAEMA) based PICM. The effect of pH on the scattering intensity and particle diameter of (▼) PEG-b-P(DEAEMA) chains (without heparin) is also shown. Arrows indicate the onset of ionization and complexation. PICM complexes were prepared as aqueous solutions with –/+ molar charge ratios of 1.5. The scattering intensity is expressed relative to the maximum scattering count observed per polymer.

Effect of Ionic Strength on Micelle Stability

It is predicted that the stability of PICM will strongly be dependent on the ionic strength of the surroundings. The presence of salts can indeed compete with the polymer–heparin electrostatic interactions, thereby destabilizing the PICM (27). The influence of salt concentration on the stability of micelles was therefore studied by measuring the scattering intensity (Fig. 7A) and size (Fig. 7B) of micelles at various NaCl concentrations. As a general trend, an increase in ionic strength was associated with a slight increase in the mean diameters of the micelles, up to NaCl concentrations of about 0.1 M. The most probable explanation is that the complexes presented a slight net charge that provided electrostatic repulsions between polymer chains and limited their self-association. Addition of salt screened these charges, reduced electrostatic repulsions and allowed for more chains to aggregate into the core of larger micelles (28). This effect was particularly pronounced for the PICM of PEG-*b*-P(DEAEMA) given that the shielded DEAEMA units are the most hydrophobic. Further increases in NaCl concentrations eventually led to decreases in both micelle size and light scattering intensity, thus indicating the dissociation of the complexes. Of all polymers, PEG-*b*-P(AEMA) was the most stable, exhibiting 94% of its initial scattering intensity under physiological isotonic conditions (0.15 M NaCl).

Effect of Freeze-Drying on PICM Integrity

It is expected that aqueous solutions of heparin-based PICM will have limited stability due to possible chemical and physical degradation processes. Lyophilization is a method of choice to grant acute stability and suitable shelf-life to labile therapeutic systems. For example, lyophilization was successfully used to store oligonucleotide–PEG-polyamine complexes without modifying the size of the complexes (29). Its effect on the integrity of PICM prepared in an acetate buffer (pH 5) was thus investigated and is summarized in Table I. It can readily be seen that the PEG-*b*-P(AEMA), PEG-*b*-P(TMAEMA), and PEG-*b*-P(DEMAEMA) complexes withstood both the freezing and drying procedures. The resuspended carriers indeed present unaltered or slightly increased diameters. The greatest impact of lyophilization lied in increased PIs for the rehydrated PICM. PEG-*b*-P(DMAEMA) and PEG-*b*-P(DEAEMA) complexes, however, did not tolerate freeze-drying as satisfactorily. Resuspended PEG-*b*-P(DMAEMA) PICM presented two populations while there was a marked precipitation of the PEG-*b*-P(DEAEMA) com-

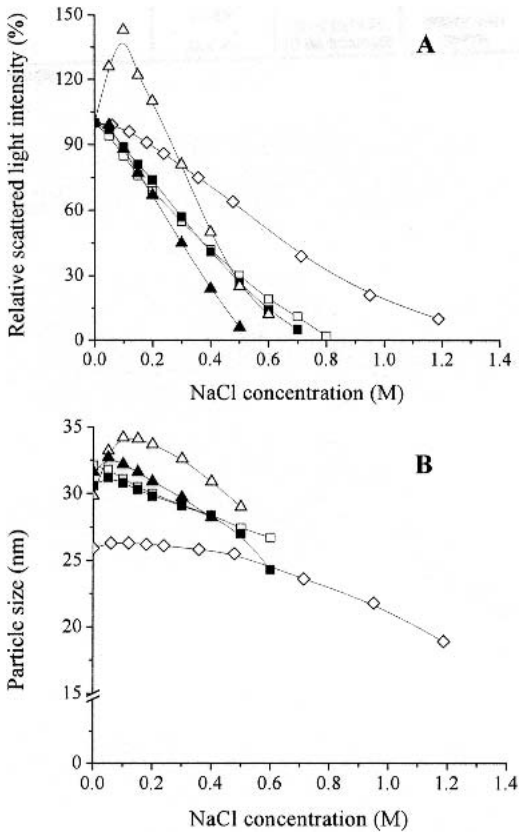

Fig. 7. Effect of ionic strength on (A) scattering intensity and (B) particle diameter of (◇) PEG-*b*-P(AEMA), (□) PEG-*b*-P(DMAEMA), (■ PEG-*b*-P(TMAEMA), (△) PEG-*b*-P(DEAEMA), and (▲) PEG-*b*-P(DEMAEMA) based PICM. Polyelectrolyte complexes were prepared as acidified aqueous solutions (pH 4) with –/+ molar charge ratios of 1. The scattering intensity is expressed relative to the initial scattering count.

plexes. This phenomenon was attributed to the presence of salts in the preparations. To illustrate this hypothesis, we prepared complexes as acidic aqueous solutions and showed that the lyophiles presented sizes and population distributions comparable to that of the mother complexes (data not shown). One possible explanation is that there is an increase in the local concentration of polymer, heparin, and buffer salts at the onset of freezing. It is known that as the preparation cools down, it reaches a temperature where pure ice first begins to crystallize out of solution and induces the isolation and concentration of the solution components (30). Increased concentrations in buffer salts can contribute to partial dehydration of the PEG corona and interpenetration of micelle cores (31), thereby accounting for the formation of larger micelles and even micellar aggregation. This mechanism is in agreement with the observation that the aggregation of the lyophiles increased with increasing hydrophobicity of the complexes.

CONCLUSIONS

ATRP was successfully used to prepare copolymers presenting primary, tertiary, and quaternary amino groups. Electrostatic interactions between the amino copolymers and heparin triggered the formation of small and monodisperse polyelectrolyte complexes with properties dependent on the substitution of their constituents. For instance, copolymers bearing primary amines were shown to form complexes under the widest pH range and to yield assemblies stable to ionic strength variations. Hydrophobicity was also shown to play a role, generally inducing the formation of complexes of larger diameters. Future studies will aim at relating the stability of the PICM to the oral bioavailability of heparin. The combination of conditions such as increases in ionic strength and basification of the surroundings as the complexes transit from the stomach to the jejunum are expected to induce the *in vivo* dissociation of the complexes (along with heparin release). Furthermore, the release profile should also be subject to extreme dilution and possible electrostatic interactions between the cationic blocks and the negatively charged intestinal mucosa and mucus.

ACKOWLEDGMENTS

Financial support from the Natural Sciences and Engineering Research Council of Canada and the Canada Research Chair Program is acknowledged. The authors extend their gratitude to Marc A. Gauthier and Marie-Christine Jones for their critical reading of the manuscript and helpful discussions.

REFERENCES

1. E. Windsor and G. E. Cronheim. Gastro-intestinal absorption of heparin and synthetic heparinoids. *Nature* **190**:263–264 (1961).
2. R. H. Engel and S. J. Riggi. Effect of sulfated and sulfonated surfactants on the intestinal absorption of heparin. *Proc. Soc. Exp. Biol. Med.* **130**:879–884 (1969).
3. Y-K. Lee, J. H. Nam, H-C. Shin, and Y. Byun. Coagulation of low-molecular-weight heparin and deoxycholic acid for the development of a new oral anticoagulant agent. *Circulation.* **104**: 3116–3120 (2001).
4. N. Sakuragawa, K. Takahashi, M. Ueno, and I. Horikoshi. Oral administration of heparin. *Acta Med. Biol.* **29**:33–37 (1981).
5. R. A. Baughman, S. C. Kapoor, R. K. Agarwal, J. Kisicki, F. Catella-Lawson, and G. A. FitzGerald. Oral delivery of anticoagulant doses of heparin. A randomized, double-blind, controlled study in humans. *Circulation.* **98**:1610–1615 (1998).
6. Y. Jiao, N. Ubrich, V. Hoffart, M. Marchand-Arvier, C. Vigneron, M. Hoffman, and P. Maincent. Anticoagulant activity of heparin following oral administration of heparin-loaded microparticles in rabbits. *J. Pharm. Sci.* **91**:760–768 (2002).
7. Y. Jiao, N. Ubrich, M. Marchand-Arvier, C. Vigneron, M. Hoffman, T. Lecompte, and P. Maincent. *In vitro* and *in vivo* evaluation of oral heparin-loaded polymeric nanoparticles in rabbits. *Circulation.* **105**:230–235 (2002).
8. K. Kataoka, A. Harada, and Y. Nagasaki. Block copolymer micelles for drug delivery: design, characterization and biological significance. *Adv. Drug Deliv. Rev.* **47**:113–131 (2001).
9. A. V. Kabanov, T. K. Bronich, V. A. Kabanov, K. Yu, and A. Eisenberg. Soluble stoichiometric complexes from poly(*N*-ethyl-4-vinylpyridinium) cations and poly(ethylene oxide)-*block*-polymethacrylate anions. *Macromolecules* **29**:6797–6802 (1996).
10. A. Harada, H. Togawa, and K. Kataoka. Physicochemical properties and nuclease resistance of antisense-oligonucleotides entrapped in the core of polyion complex micelles composed of poly(ethylene glycol)-poly(L-lysine) block copolymers. *Eur. J. Pharm. Sci.* **13**:35–42 (2001).
11. K. Kataoka, H. Togawa, A. Harada, K. Yasugi, T. Matsumoto, and S. Katayose. Spontaneous formation of polyion complexe micelles with narrow distribution from antisense oligonucleotide and cationic block copolymer in physiological saline. *Macromolecules* **29**:8556–8557 (1996).
12. Y. Kakizawa and K. Kataoka. Block copolymer micelles for delivery of gene and related compounds. *Adv. Drug Deliv. Rev.* **54**:203–222 (2002).
13. A. Harada and K. Kataoka. Novel polyion complex micelles entrapping enzyme molecules in the core: preparation of narrowly-distributed micelles from lysosyme and poly(ethylene glycol)-poly(aspartic acid) block copolymer in aqueous medium. *Macromolecules* **31**:288–294 (1998).
14. O. Boussif, F. Lezoualc'h, M. A. Zanta, M. D. Mergny, D. Scherman, B. Demeneix, and J-P. Behr. A versatile vector for gene and oligonucleotide transfer into cells in culture and *in vivo*: polyethylenimine. *Proc. Natl. Acad. Sci. U. S. A.* **92**:7297–7301 (1995).
15. J. F. Kukowska-Latallo, A. U. Bielinska, J. Johnson, R. Spindler, D. A. Tomalia, and J. R. Baker, Jr. Efficient transfer of genetic material into mammalian cells using starburst polyamidoamine dendrimers. *Proc. Natl. Acad. Sci. U. S. A.* **93**:4897–4902 (1996).
16. U. Rungsardthong, M. Deshpande, L. Bailey, M. Vamvakaki, S. P. Armes, M. C. Garnett, and S. Stolnik. Copolymers of amine methacrylate with poly(ethylene glycol) as vectors for gene therapy. *J. Controlled Release* **73**:359–380 (2001).
17. K. A. Davis and K. Matyjaszewski. ABC triblock copolymers prepared using atom transfer radical polymerization techniques. *Macromolecules* **34**:2101–2107 (2001).
18. S. Angot, D. Taton, and Y. Gnanou. Amphiphilic stars and dendrimer-like architectures based on poly(ethylene oxide) and polystyrene. *Macromolecules* **33**:5418–5426 (2000).
19. V. Coessens and K. Matyjaszewski. Synthesis of polymers with amino end groups by atom transfer radical polymerization. *J. Macromol. Sci. Pure Appl. Chem.* **A36**:811–826 (1999).
20. K. Matyjaszewski. Mechanistic and synthetic aspects of atom transfer radical polymerization. *J. Macromol. Sci. Pure Appl. Chem.* **A34**:1785–1801 (1997).
21. V. Coessens, T. Pintauer, and K. Matyjaszewski. Functional polymers by atom transfer radical polymerization. *Prog. Polym. Sci.* **26**:337–377 (2001).
22. M. Ranger, M-C. Jones, M-A. Yessine, and J-C. Leroux. From well-defined diblock copolymers prepared by a versatile atom transfer radical polymerization method to supramolecular assemblies. *J. Polym. Sci. A: Polym. Chem.* **39**:3861–3874 (2001).
23. A. S. Lee, A. P. Gast, V. Bütün, and S. P. Armes. Characterizing the structure of pH dependent polyelectrolyte block copolymer micelles. *Macromolecules* **32**:4302–4310 (1999).
24. K. Matyjaszewski, B. Göbelt, H-J. Paik, and C. P. Horwitz. Tridendate nitrogen-based ligands in Cu-based ATRP: a structure-activity study. *Macromolecules* **34**:430–440 (2001).
25. M. Přádný and S. Ševčík. Precursors of hydrophilic polymers, 3[a)]

The potentiometric behavior of isotactic and atactic poly(2-dimethylaminoethyl methacrylate) in water/ethanol solutions. *Makromol. Chem.* **186**:111–121 (1985).
26. H. M. Wang, D. Loganathan, and R. J. Linhardt. Determination of the pK_a of gluronic acid and the carboxy groups of heparin by ^{13}C-nuclear-magnetic-resonance spectroscopy. *Biochem. J.* **278**: 689–695 (1991).
27. A. Harada and K. Kataoka. Formation of stable and monodispersive polyion complex micelles in aqueous medium from poly(L-lysine) and poly(ethylene glycol)-poly(aspartic acid) block copolymer. *J. Macromol. Sci. Pure Appl. Chem.* **A34**:2119–2133 (1997).
28. A. S. Lee, V. Bütün, M. Vamvakaki, S. P. Armes, J. A. Pople, and A. P. Gast. Structure of pH-dependent block copolymer micelles: charge and ionic strength dependence. *Macromolecules* **35**:8540–8551 (2002).
29. S. V. Vinogradov, T. K. Bronich, and A. V. Kabanov. Self-assembly of polyamine-poly(ethylene glycol) copolymers with phosphorothioate oligonucleotides. *Bioconjug. Chem.* **9**:805–812 (1998).
30. T. W. Randolph. Phase separation of excipients during lyophilization: effects on protein stability. *J. Pharm. Sci.* **86**:1198–1203 (1997).
31. N. J. Jain, V. K. Aswal, P. S. Goyal, and P. Bahadur. Salt induced micellization and micelle structures of PEO/PPO/PEO block copolymers in aqueous solution. *Colloids Surf. A: Physicochem. Eng. Asp.* **173**:85–94 (2000).